# Optimization of Spectrum Efficiency in UAV Cognitive Communication Network Based on Trajectory Planning

Yilong Gu*
Graduate School, Air Force Engineering University
gu356505504@463.com

Yangchao Huang
College of Information and Navigation, Air Force Engineering University
gxyxhbwhyc@sohu.com

Yuetong Zhang
College of Information and Navigation, Air Force Engineering University
356505504@qq.com

Qi An
Graduate School, Air Force Engineering University
ann1278067675@163.com

Huizhu Han
Graduate School, Air Force Engineering University
h18137682630@163.com

Youbin Fu
Graduate School, Air Force Engineering University
fyb6563@163.com

Yanhui Zhang
Graduate School, Air Force Engineering University
1105406986@qq.com

## ABSTRACT

In order to solve the shortage of spectrum resources and improve the spectrum efficiency (SE) in unmanned aerial vehicle (UAV) cognitive communication network, this paper optimizes the sensing radian and UAV's real-time trajectory from the perspective of time and space resource allocation. Firstly, the sensing radian is optimized to maximize throughput. Secondly, under the constraints of the primary user (PU) interference threshold, the maximum speed of UAV, the initial and terminal positions of UAV, the flight trajectory of UAV is optimized in real time by iteration algorithm to maximize the throughput. Finally, the SE optimization algorithm based on sensing radian allocation and trajectory planning for UAV cognitive communication is proposed. Simulation results show that the proposed algorithm is effective and better than existing schemes.

## CCS CONCEPTS

• **Networks**; • **Network components**; • **Wireless access points, base stations and infrastructure**; • **Cognitive radios**;

## KEYWORDS

unmanned air vehicle, spectrum efficiency, trajectory, sensing radian

**ACM Reference Format:**
Yilong Gu, Yangchao Huang, Yuetong Zhang, Qi An, Huizhu Han, Youbin Fu, and Yanhui Zhang. 2021. Optimization of Spectrum Efficiency in UAV Cognitive Communication Network Based on Trajectory Planning. In *2021 the 11th International Conference on Communication and Network Security (ICCNS) (ICCNS 2021), December 03–05, 2021, Weihai, China.* ACM, New York, NY, USA, 8 pages. https://doi.org/10.1145/3507509.3507514


*ICCNS 2021, December 03–05, 2021, Weihai, China*

ACM ISBN 978-1-4503-8642-5/21/12…$15.00
https://doi.org/10.1145/3507509.3507514

## 1 INTRODUCTION

Due to the characteristics of high mobility, low cost and flexible deployment of UAV, it has been widely used in different fields in recent years. In order to support more and more applications of UAV in the future, more stringent requirements on the communication performance of UAV are put forward [1]. However, the available spectrum resources for UAV are limited [2], which leads to many challenges for the development of UAV communication. In order to solve this problem, cognitive radio (CR) technology is considered as an effective scheme [3]. UAV communication network combined with CR has great potential in improving SE and has been extensively studied by scholars [4-6].

In CR, sensing reliability and effective transmission rate are determined by the allocation of time resources in the process of transmission and sensing. In the case of limited time resources, with the increase of sensing time, the reliability of sensing becomes higher, but the data transmission time becomes shorter. Therefore, the research on time resource allocation in cognitive UAV communication network is an important method to maximize UAV throughput [7].

Compared with the traditional CR network [8], the mobility of UAV can be used to improve the performance of cognitive communication. On the one hand, the transmission rate of wireless communication is affected by the channel quality, and the distance and path loss between communication points determine the quality of ground to air channel. Because UAV communication can avoid the shielding effects of mountains and buildings in the communication process, the channel quality between UAV and ground node is better than the channel quality between ground node and ground node in general. On the other hand, when the distance between UAV and primary transmitter (PT) is reduced, the perceived reliability is improved; When the distance between UAV and Sr decreases, the

transmission rate increases. However, when the distance between UAV and primary receiver (PR) is small, the secondary communication link may cause greater interference to PR. Therefore, the distance between UAV and different ground nodes has an important impact on improving the SE of UAV cognitive communication network.

At present, there has been a lot of research on UAV trajectory planning and SE optimization. In [9, 10], the joint optimization of UAV trajectory and power resource allocation to maximize throughput is studied, but the influence of the SE by sensing time is not considered. In [11], the joint optimization of UAV transmission power and spectrum sensing time to achieve the maximum SE and EE is studied under the condition that the position information of UAV is fixed. In [12], the authors consider the spectrum sensing problem in UAV straight flight scene and UAV circular flight scene to maximize the effective throughput of UAV by optimizing the sensing radian under the constraint of interference throughput. However, the influence of UAV's irregular flight on SE has not been considered in references [11–13]. In reference [14], the trajectory of UAV is jointly optimized to improve throughput. However, it can only plan the trajectory in the whole flight cycle based on the information of the starting time, and has poor adaptability to the frequent switching of busy and idle states of the primary user (PU) network.

In this paper, the trajectory of UAV is planned in real time to adapt to the frequent switching of busy and idle state of PU network, and the throughput improvement scheme is studied under the constraints of PU interference threshold, maximum speed of UAV, initial and terminal positions of UAV in UAV cognitive communication network. Finally, the algorithm based on the sensing radian allocation and trajectory planning of UAV cognitive communication is proposed to improve throughput. The simulation results show that the proposed algorithm is better than the existing schemes, which proves the effectiveness of the proposed algorithm.

## 2 SYSTEM MODEL

The UAV cognitive communication network model is shown in Figure 1 (a), which consists of a PT, a PR, an UAV with cognitive function and M Secondary Receivers (SR). The UAV with cognitive function flies around the PT to perform reconnaissance and detection tasks, senses the PU status in real time, and communicates with the SR opportunistically using the PT spectrum.

### 2.1 Coordinate system and channel model

In this paper, a three-dimensional Cartesian coordinate system is used. In the coordinate system, suppose that the positions of PT, PR and SRs are fixed. The horizontal position of PT is $\mathbf{O} = (x_0, y_0)$, and the position of PR is $\mathbf{Z} = (z_x, z_y)$. The i-th $SR$ is represented by $SR_i$, which horizontal position is $\mathbf{S}_i = ({s_x}^i, {s_y}^i)$ , where $i = 1, 2...M$. Assuming that the horizontal position of the UAV will change with time at a fixed height $H$, and the horizontal is $q(t) = (q_x(t), q_y(t))$. Let $\widehat{v}_{\max}$ denote the maximum velocity of the UAV, $q_x(t)'$and $q_y(t)'$be the first derivative of $q_x(t)$and$q_y(t)$, then we have$\sqrt{{q_x}^2(t)' + {q_y}^2(t)'} \leq v_{\max}$.

It is assumed that the time of UAV flying over radian $2\pi$ as a period $T$, and a period is divided into$N$equal flight time slots $T_c$. In order to facilitate the study of the characteristics of UAV circling flight, let the flight time slots $.T_c$. corresponding to the UAV flying over radian $\theta$, then we have $N\theta$=$2\pi$. As shown in Figure 1 (b), when UAV flying over radian $K\theta$, the flight radius of the UAV is set as $d_K$, and the horizontal position of the UAV is $\mathbf{q}(K) = ({q_x}^K, {q_y}^K)$, where $K = 0, 1, 2, \cdot s, N$. Suppose that the initial flight radius of the UAV is $d_0$, and the initial horizontal position is $\mathbf{q}(0) = (x_0, y_0 + d_0)$, then we can obtain:

$$\mathbf{q}_x{}^K = x_0 + d_K \sin(K\theta) \tag{1}$$

$$\mathbf{q}_y{}^K = y_0 + d_K \cos(K\theta) \tag{2}$$

Assuming that the UAV will return to $\mathbf{q}(0)$ after a period, and the minimum distance between the UAV and the PT is $d_{sa}$, Thus, we can obtain the constraint of the UAV flight trajectory:

$$\|\mathbf{q}(K) - \mathbf{q}(K-1)\|^2 \leq (v_{\max} T_c)^2 \tag{3}$$

$$\mathbf{q}(0) = \mathbf{q}(N) \tag{4}$$

$$\|\mathbf{q}(K) - \mathbf{O}\|^2 \geq {d_{sa}}^2 \tag{5}$$

where $\|\cdot\|$ is the Euclidean norm.

When the UAV is in position $\mathbf{q}(K)$, its distances from PT, PR and $SR_i$ are $\sqrt{H^2 + \|\mathbf{q}(K) - \mathbf{O}\|^2}$,$\sqrt{H^2 + \|\mathbf{q}(K) - \mathbf{Z}\|^2}$,$\sqrt{H^2 + \|\mathbf{q}(K) - \mathbf{S}_i\|^2}$. Assuming that the communication link between the UAV and ground node is line-of-sight link, the channel power gain between the UAV and the PT, PR and $SR_i$ can be expressed as:

$$\beta_{PT} = \frac{\beta_0}{(H^2 + \|\mathbf{q}(K) - \mathbf{O}\|^2)} \tag{6}$$

$$\beta_{PR} = \frac{\beta_0}{(H^2 + \|\mathbf{q}(K) - \mathbf{Z}\|^2)} \tag{7}$$

$$\beta_{SRi} = \frac{\beta_0}{(H^2 + \|\mathbf{q}(K) - \mathbf{S}_i\|^2)} \tag{8}$$

where $\beta_0$ represents the power gain of the channel at a reference distance of 1 meter.

### 2.2 Spectrum sensing model

As shown in Figure 2, it is composed of sensing radian and transmission radian. Within the sensing radian $\theta_s$, the UAV senses whether the PT is active, and within $\theta - \theta_s$, the UAV opportunistically uses the spectrum to transmit data. At time slot K, the sensing time is $\tau_s = \frac{\theta_s T_c}{\theta}$.

Assuming that the UAV uses the energy detection method to detect whether the PT is active, the signal received by the UAV is:

$$Y(j) = \omega \chi_{pt}(j) \beta_{PT}(j) + \chi_n(j), j = 1, 2, \ldots, L \tag{9}$$

where $\omega = 0$ indicates that the PT is idle, and $\omega = 1$ indicates that the PT is active. $\chi_{pt}$ is the signal transmitted by the PT, $\chi_n$ is the noise received by the UAV, $L = \sqrt{\tau_s f_s}$ is the number of sampling points, and $f_s$ indicates the sampling frequency. The energy statistic of the$Y(j)$ is $E(Y) = \frac{1}{L}\sum_{j=1}^{L} |Y(j)|^2$, when L is large enough, $Y(j)$ obeys the Gaussian distribution. Therefore, the false alarm probability can be expressed as [15]

$$P_f = Q(\sqrt{2\gamma + 1} Q^{-1}(\bar{P}_d) + \sqrt{\frac{\theta_s T_c}{\theta} f_s \gamma}) \tag{10}$$

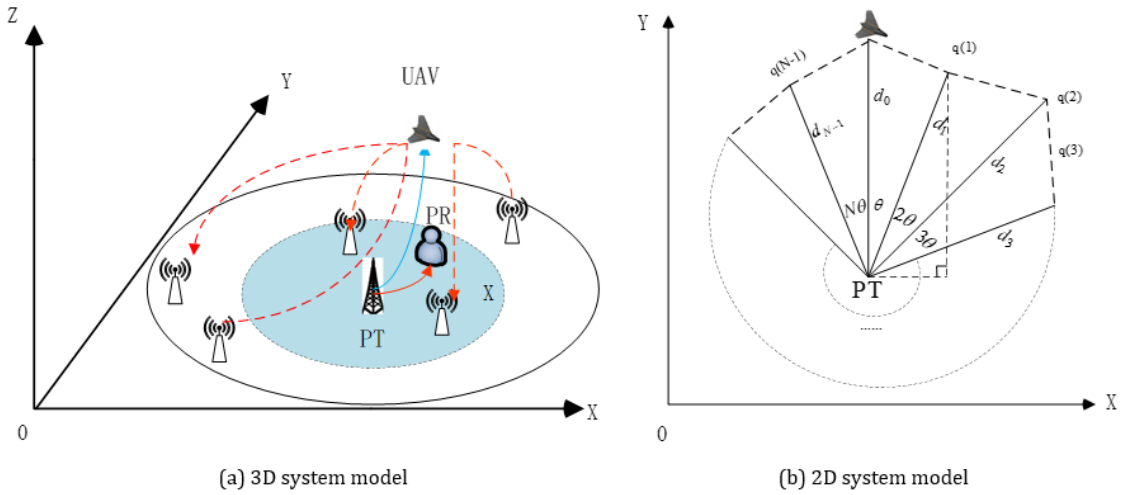


**Figure 1: UAV cognitive communication network system model**

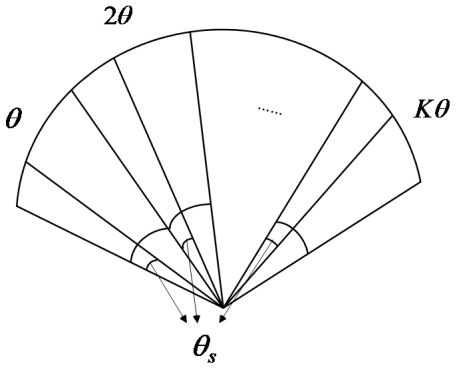


**Figure 2: Spectrum sensing model of UAV cognitive communication**

where$Q(x) = \frac{1}{\sqrt{2\pi}} \int_x^{\infty} \exp(-\frac{t^2}{2})dt$ is Gaussian distribution function, $\gamma$ denotes the sensing signal-to-noise ratio, and $\bar{P}_d$ is the target detection probability. In the time slot K, when the PT is idle, the transmission rate between the UAV and the $SR_i$ can be expressed as:

$$C_{i0}(K) = \log_2(1 + \frac{\beta_0 P_u}{(H^2 + \|\mathbf{q}(K) - \mathbf{S}_i\|^2)\sigma^2}) \tag{11}$$

where $P_u$ is the transmit power of the UAV communication, and the $\sigma^2$ is noise variance. When the PT is active, the transmission rate between the UAV and the $SR_i$can be expressed as:

$$C_{i1}(K) = \log_2(1 + \frac{\beta_0 P_u}{(H^2 + \|\mathbf{q}(K) - \mathbf{S}_i\|^2)(\sigma^2 + P_p)}) \tag{12}$$

where $P_P$ denotes the interference power generated by the PU to the secondary communication.

As a secondary user communication, UAV can be divided into the following two situations:

(1) When the status of the PT is inactive, the UAV sensing result also shows that the spectrum is inactive, the throughput of the secondary communication link between the UAV and $SR_i$ is

$$R_{i0}{}^K = \frac{\theta - \theta_s}{\theta} P(H_0)(1 - p_f)C_{i0}(K) \tag{13}$$

where $P(H_0)$ is the inactive probability of PT.

(2) When the status of the PT is active, but the UAV sensing result shows that the spectrum is inactive, the throughput of the secondary communication link between the UAV and $SR_i$ is

$$R_{i1}{}^K = \frac{\theta - \theta_s}{\theta} P(H_1)(1 - \bar{P}_d)C_{i1}(K) \tag{14}$$

where $P(H_1)$ is the active probability of PT.

The average throughput of the UAV as a secondary user is defined as $R_i(K)$, we have $R_i{}^K = R_{i0}{}^K + R_{i1}{}^K$. When the UAV fails to detect that the ground base station is active, which will cause interference to the PU. Therefore, the value of $C_{i1}(K)$ will be less than $C_{i0}(K)$, and even the ground node will not be able to decode the information transmitted by the UAV. Therefore, the $R_i(K)$ can be approximate estimate:

$$R_i{}^K = \frac{\theta - \theta_s}{\theta}(1 - p_f)P(H_0)C_{i0}(K) \tag{15}$$

To protect the PU communication, we define the PR tolerable interference threshold generated by UAV secondary communication as $\Gamma_K$, then we have

$$\frac{\beta_0 P_u}{(H^2 + \|\mathbf{q}(K) - \mathbf{Z}\|^2)} \leq \Gamma_K \tag{16}$$

When UAV sensing that the PU is inactive, The UAV trajectory and sensing radian are optimized so that the UAV can transmit information to SR in real time with the maximum throughput, and avoid the UAV unable to communicate due to the limitation of $\Gamma_K$. From the expressions (3), (4), (5) and (16), we know that the UAV's trajectory information is a function of $d_K$. Define$R^K = \sum_{i=1}^{M} R_i{}^K$, then

this optimization problem is described as

$$\begin{aligned} (OP): &\max_{\{d_K,\theta_s\}} R^K \\ s.t: &\|\mathbf{q}(K)-\mathbf{q}(K-1)\|^2 \le (v_{\max}T_c)^2 \\ &\mathbf{q}(0)=\mathbf{q}(N) \\ &\|\mathbf{q}(K)-\mathbf{O}\|^2 \ge {d_{sa}}^2 \\ &\frac{\beta_0 P_u}{(H^2+\|\mathbf{q}(K)-\mathbf{Z}\|^2)} \le \Gamma_K \\ &0<\theta_s<\theta \end{aligned} \tag{17}$$

## 3 SOLUTIONS OF OPTIMIZATION PROBLEM

In the objective function $OP$, $C_{i0}(K)$ is determined by $d_K$ and $\theta_s$ only affects the first two terms of (15). Therefore, we divide $OP$ into two subproblems with $d_K$and $\theta_s$ as variables:

$$\begin{aligned} (OP_1): &\max_{\{\theta_s\}} \sum_{i=1}^{M} {R_i}^K \\ s.t: &\ 0<\theta_s<\theta \end{aligned} \tag{18}$$

$$\begin{aligned} (OP_2): &\max_{\{d_K\}} \sum_{i=1}^{M} {R_i}^K \\ s.t: &\|\mathbf{q}(K)-\mathbf{q}(K-1)\|^2 \le (v_{\max}T_c)^2 \\ &\mathbf{q}(0)=\mathbf{q}(N) \\ &\|\mathbf{q}(K)-\mathbf{O}\|^2 \ge {d_{sa}}^2 \\ &\frac{\beta_0 P_u}{(H^2+\|\mathbf{q}(K)-\mathbf{Z}\|^2)} \le \Gamma_K \end{aligned} \tag{19}$$

### 3.1 Optimization of sensing radian

According to (10) and (13), we know that $\theta_s$ is not affected by the value of $i$ and $K$. Therefore, the subproblem $OP_1$ can be simplified as follows

$$\begin{aligned} (OP_3): &\max_{\{\theta_s\}} {R_i}^K \\ s.t: &\ 0<\theta_s<\theta \end{aligned} \tag{20}$$

Then, the first derivative of $R_i^K$ is

$$\begin{aligned} \frac{\partial {R_i}^K}{\partial \theta_s} = C_{i0}(K)P(H_0)\Bigg[&\frac{\gamma(\theta-\theta_s)\sqrt{f_s\frac{T_c}{\theta}}}{2\sqrt{2\pi\theta_s}} \\ &\exp\Big(-\frac{(\alpha+\sqrt{\frac{\theta_s T_c}{\theta}f_s}\gamma)^2}{2}\Big)\Big) + \frac{Q(\alpha+\sqrt{\frac{\theta_s T_c}{\theta}f_s}\gamma)-1}{\theta}\Bigg] \end{aligned} \tag{21}$$

where $\alpha=\sqrt{2\gamma+1}Q^{-1}(\bar{P}_d)$. According to (21), we have

$$\lim_{\theta_s\to 0}\frac{\partial {R_i}^K}{\partial \theta_s} = +\infty \tag{22}$$

Because $Q(x)$ is a decreasing function that no more than 1, then, we can obtain that

$$\lim_{\theta_s\to \theta}\frac{\partial {R_i}^K}{\partial \theta_s} < 0 \tag{23}$$

By taking the second derivative of ${R_i}^K$, we have

$$\begin{aligned} \frac{\partial^2 {R_i}^K}{\partial {\theta_s}^2}\frac{1}{C_{i0}(K)P(H_0)} = &-\frac{\gamma\sqrt{f_s\frac{T_c}{\theta}}}{2\sqrt{2\pi}}\Bigg((\tfrac{1}{2}\theta\frac{1}{\sqrt{{\theta_s}^3}}+\frac{1}{2\sqrt{\theta_s}})\exp(-\frac{(\alpha+\sqrt{\frac{\theta_s T_c}{\theta}f_s}\gamma)^2}{2})\Bigg) \\ &-\frac{\gamma^2 f_s\frac{T_c}{\theta}}{4\sqrt{2\pi}\theta_s}(\theta-\theta_s)\exp(-\frac{(\alpha+\sqrt{\frac{\theta_s T_c}{\theta}f_s}\gamma)^2}{2})(\alpha+\sqrt{\frac{\theta_s T_c}{\theta}f_s}\gamma) \\ &-\frac{\gamma\sqrt{f_s\frac{T_c}{\theta}}}{2\theta\sqrt{\theta_s}}\exp(-\frac{(\alpha+\sqrt{\frac{\theta_s T_c}{\theta}f_s}\gamma)^2}{2}) \end{aligned} \tag{24}$$

It is easy to verify that $\frac{\partial^2 {R_i}^K}{\partial {\theta_s}^2} < 0$ for $0<\theta_s<\theta$, so we can obtain that $\frac{\partial {R_i}^K}{\partial \theta_s}$ is a monotonically decreasing function for this interval. According to (22) and (23), it is shown that ${R_i}^K$ increases when $\theta_s$ is small and decreases when $\theta_s$ approaches $\theta$. Hence, there is an optimal $\theta_s$ to maximize ${R_i}^K$ within interval $(0,\theta)$. Define this optimal $\theta_s$ as ${\theta_s}^*$, which can be efficiently solved by the binary method.

### 3.2 Optimization of trajectory

The first derivative of ${R_i}^K$ with respect to $d_K$ is

$$\begin{aligned} \frac{\partial {R_i}^K}{\partial d_K} = &\frac{-2\beta_0 P_u\sigma^2\left[d_K+\sin(K\theta)(x_0-{s_x}^i)+\cos(K\theta)(y_0-{s_y}^i)\right]}{\left\{\beta_0 P_u+\sigma^2\left[H^2+(x_0+d_K\sin(K\theta)-{s_x}^i)^2+(y_0+d_K\cos(K\theta)-{s_y}^i)^2\right]\right\}} \\ &\times\frac{\frac{\theta-\theta_s}{\theta}P(H_0)(1-p_f)}{\ln 2\sigma^2\left[H^2+(x_0+d_K\sin(K\theta))^2+(y_0+d_K\cos(K\theta))^2\right]} \end{aligned} \tag{25}$$

If $d_K < -(\sin(K\theta)(x_0-{s_x}^i)+\cos(K\theta)(y_0-{s_y}^i))$, we have $\frac{\partial R_i(K)}{\partial d_K} > 0$, then ${R_i}^K$ is a increasing function; if $d_K > -(\sin(K\theta)(x_0-{s_x}^i)+\cos(K\theta)(y_0-{s_y}^i))$, we have $\frac{\partial R_i(K)}{\partial d_K} < 0$, then ${R_i}^K$ is a decreasing function. In a word, ${R_i}^K$ is the single-peaked function, and we can obtain the maximum value when $d_K=-(\sin(K\theta)(x_0-{s_x}^i)+\cos(K\theta)(y_0-{s_y}^i))$. Denote:

$$d_{K1}=\min_i(-(\sin(K\theta)(x_0-{s_x}^i)+\cos(K\theta)(y_0-{s_y}^i))) \tag{26}$$

$$d_{K2}=\max_i(-(\sin(K\theta)(x_0-{s_x}^i)+\cos(K\theta)(y_0-{s_y}^i))) \tag{27}$$

then $R(K)$ is a monotonically decreasing function for $d_K < d_{K1}$, and $R(K)$ is a monotonically increasing function for $d_K > d_{K2}$. Therefore, the maximum value of $R(K)$ can be obtained in the interval$[d_{K1}, d_{K2}]$.

According to (1), (2) and (3), we have

$${d_{K-1}}^2+{d_K}^2-2d_{K-1}d_K\cos(\theta) < {v_{\max}}^2{T_c}^2 \tag{28}$$

It can be known that $\mathbf{O}$, $\mathbf{q}(K)$ and $\mathbf{q}(K-1)$ form a closed triangle, so ${d_{K-1}}^2+{d_K}^2-2d_{K-1}d_K\cos(\theta)={v_{\max}}^2{T_c}^2$ must have real roots, and the two roots of the equation ${d_{K-1}}^2+{d_K}^2-2d_{K-1}d_K\cos(\theta)-{v_{\max}}^2{T_c}^2=0$ are as follows

$$d_{K1}=d_{K-1}\cos(\theta)-\sqrt{v^2-d_{K-1}\sin^2(\theta)} \tag{29}$$

$$d_{K2}=d_{K-1}\cos(\theta)+\sqrt{v^2-d_{K-1}\sin^2(\theta)} \tag{30}$$

The minimum flight radius of the UAV is defined as $d_{K\min}$and the maximum flight radius is defined as $d_{K\max}$. According to (5), we have $d_{K\min}$=$d_{K1}$, $d_{K\max}$=$d_{K2}$ when $d_{K1} \ge d_{sa}$;$d_{K\min}$=$d_{sa}$, $d_{K\min}$=$d_{sa}$ when $d_{K1} < d_{sa}$.Note that, if $d_{sa} > d_{K2}$, the UAV will not be able to fly according to (5). Therefore, we obtain the range of $d_K$ as $\mathbf{D}=(d_{K\min}, d_{K\max})$.

According to (1), (2) and (16), we can obtain

$$ad_K{}^2 + bd_K + c \geq 0 \tag{31}$$

Where $a = 1$, $b = 2(\sin(K\theta)(x_0 - z_x) + \cos(K\theta)(y_0 - z_y))$, $c = (x_0 - z_x)^2 + (y_0 - z_y)^2 + H^2 - \frac{\beta_0 P_u}{\Gamma_K}$.

When $b^2 - 4ac \leq 0$, the (16) always satisfies the condition for any $d_K$, therefore, the constraint range of $d_K$ is $\mathfrak{R} = (d_l, d_r) = (d_{K\min}, d_{K\max})$.

When $b^2 - 4ac > 0$, the two roots of $ad_K{}^2 + bd_K + c = 0$ are $d_{K3} = \frac{-b-\sqrt{b^2-4ac}}{2a}$ and $d_{K4} = \frac{-b+\sqrt{b^2-4ac}}{2a}$. Then the range of $d_K$ satisfying constraint (16) are $(-\infty, d_{K3})$ and $(d_{K4}, +\infty)$, the specific trajectory optimization is shown in Algorithm 1 and 2.

**Algorithm 1** Solve $\theta^*$ by Binary Method

Initialize K=1; i=1; tolerance level $\varpi$,
$\theta_l = 0, \theta_r = \theta, \theta_m = (\theta_l + \theta_r)/2$, calculate ${R_i}^K(\theta_l)$ and ${R_i}^K(\theta_r)$, ${R_i}^K(\theta_m)$, define $\frac{\partial {R_i}^K}{\partial \theta_s} = R_i^{K'}$.
Repeat
If $R_i^{K'}(\theta_l) < 0$
$\theta_r \leftarrow \theta_m$;
calculate ${R_i}^K(\theta_r)$;
End
else if $R_i^{K'}(\theta_l) > 0$
$\theta_l \leftarrow \theta_m$;
calculate ${R_i}^K(\theta_l)$;
End
calculate $\theta_m = (\theta_l + \theta_r)/2$和${R_i}^K(\theta_m)$;
calculate $R_i^{K'}(\theta_m)$;
Until $|{R_i}^{K'}(\theta_m)| \leq \varpi$;
Output: $\theta^* \leftarrow \theta_m$。

## 4 NUMERICAL RESULTS

In this section, we verify the effectiveness of the proposed algorithm by simulation experiments. Suppose all the ground nodes are distributed in the region of $2000 \times 2000\text{m}^2$, set **O** as (1000m, 1000m), and **Z** as(1400m, 800m). The coordinates of SR are $(1800, 600)$, $(220, 1260)$, $(850, 1600)$, $(1500, 1400)$, $(250, 1500)$, $(400, 1600)$, and $(600, 700)$. The specific simulation parameters are shown in Table 1

Figure 3 shows the curve of the variation of $R^K$ with $\theta_s$. With the increasing of $\theta_s$, $R^K$ shows an increasing trend followed by a decreasing trend, and there is an optimal $\theta_s$ to maximize $R^K$. From the Figure 3, the increase in $\theta_s$ first improves the sensing performance, leading to throughput increase, however, as the value of $\theta_s$ increases further, the transmission radian will gradually become smaller, then the value of $R^K$ goes down. When K is taken to different values, the optimal sensing time of the three curves is the same value, which is consistent with the analysis in this paper. Therefore, the throughput within any flight radian K is maximum when taken$\theta_s$=${\theta_s}^*$.

Figure 4 shows the trajectory of two flight scenarios with initial flight radius $d_0$=400m. In the fixed radius flight scenario, the UAV will always fly around the PT at the flight radius $d_K = d_0$. In the proposed scheme, the trajectory of the UAV is flown in the direction away from the PR to minimize the interference with the

**Algorithm 2** SE improvement by trajectory optimization

Initialize
$N;M;H;v_{\max};T;\theta{=}2\pi/N;d_{sa};d_0;\beta_0;P_u;\sigma^2;\gamma;\bar{P}_d;P(H_0);f_s$;according to Algorithm 1, calculate $\theta^*$;
for K=1 to N
(1) calculate $d_{K1}$, $d_{K2}$, $d_1$, $d_2$;
(2) if $d_1 \geq d_{sa}$
$d_{K\min}{=}d_1$, $d_{K\max}{=}d_2$;
elseif $d_1 < d_{sa}$
$d_{K\min}{=}d_{sa}$, $d_{K\max}{=}d_2$;
End
(3) according to (31), calculate $b^2 - 4ac$;
(4) if $b^2 - 4ac \leq 0$
$\mathfrak{R} = (d_l, d_r) = (d_{K\min}, d_{K\max})$;
else
$d_{K3} = \frac{-b-\sqrt{b^2-4ac}}{2a}$,$d_{K4} = \frac{-b+\sqrt{b^2-4ac}}{2a}$;
if $d_{K\max} \leq d_{K3}$ or $d_{K\min} \geq d_{K4}$
$\mathfrak{R} = (d_l, d_r) = (d_{K\min}, d_{K\max})$;
elseif $d_{K\min} < d_{K3} < d_{K\max} < d_{K4}$
$\mathfrak{R} = (d_l, d_r) = (d_{K\min}, d_{K3})$;
elseif $d_{K3} < d_{K\min} < d_{K4} < d_{K\max}$
$\mathfrak{R} = (d_l, d_r) = (d_{K4}, d_{K\max})$;
elseif $d_{K\min} < d_{K3} < d_{K4} < d_{K\max}$
$\mathfrak{R} = (d_{K\min}, d_{K3}) \bigcup (d_{K4}, d_{K\max})$;
elseif $d_{K3} < d_{K\min} < d_{K\max} < d_{K4}$
$d_K = d_{K-1}$,${R^K}_{\max} = 0$, do step (8);
End
(5) $\mathfrak{I} = \mathfrak{R} \cap (d_{K1}, d_{K2})$;
if $\mathfrak{I}$ is empty
$\mathfrak{I} = \mathfrak{R}$;
end
(6) solve the ${d_K}^{opt}$ in $\mathfrak{I}$ by exhaustive search;
(7) ${R^K}_{\max} = R^K(\theta^*, {d_K}^{opt})$,$d_K = {d_K}^{opt}$,$d_N = d_0$;
(8) according to (1) and (2), calculate ${\mathbf{q}_x}^K$ and ${\mathbf{q}_y}^K$;
(9) output:$\theta^*$, $d_K$, ${\mathbf{q}_x}^K$, ${\mathbf{q}_y}^K$, ${R^K}_{\max}$;
(10) $d_N = d_0$;
End

**Table 1: Parameters in numerical analysis**

| Parameter | Value | Parameter | Value |
|---|---|---|---|
| $N$ | 80 | $M$ | 7 |
| $H$(m) | 100 | $v_{\max}$(m/s) | 20 |
| $d_{sa}(m)$ | 100 | $\sigma^2$(dBm) | -150 |
| $P(H_0)$ | 0.7 | $\overline{P_d}$ | 0.9 |
| $\gamma(dB)$ | -20 | $f_s$(MHz) | 6 |
| $P_u$(W) | 1 | $\Gamma_K(dBm)$ | -50 |

PR. As $d_K$ decreases to $d_{sa}$, the UAV will continue to fly with $d_{sa}$ as its radius. After the UAV gradually moves away from the PR, $d_K$ keeps increasing and tends to fly closer to the SR to increase the throughput.

Figure 5 shows the changing curves of the maximum throughput with the flight radian for different signal-to-noise ratios. From figure. 4, it can be seen that when the UAV is close to the PR, ${R^K}_{\max}$ will be

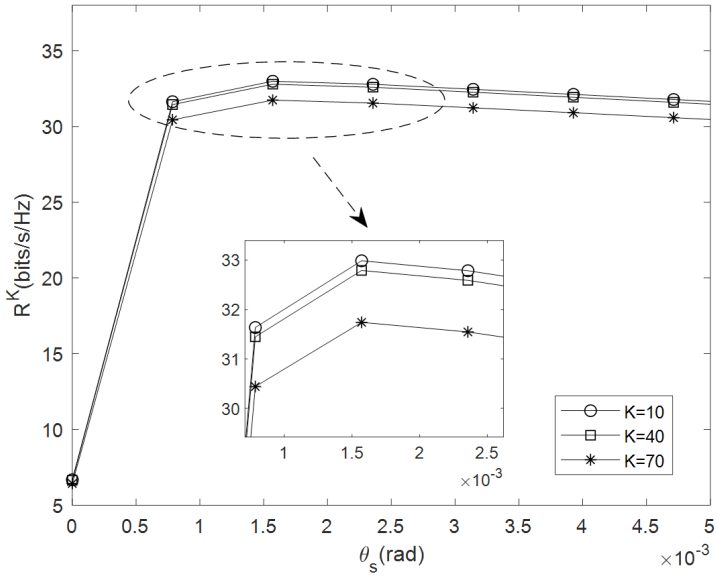


**Figure 3: $R^K$ vs $\theta_s$ under different $K$**

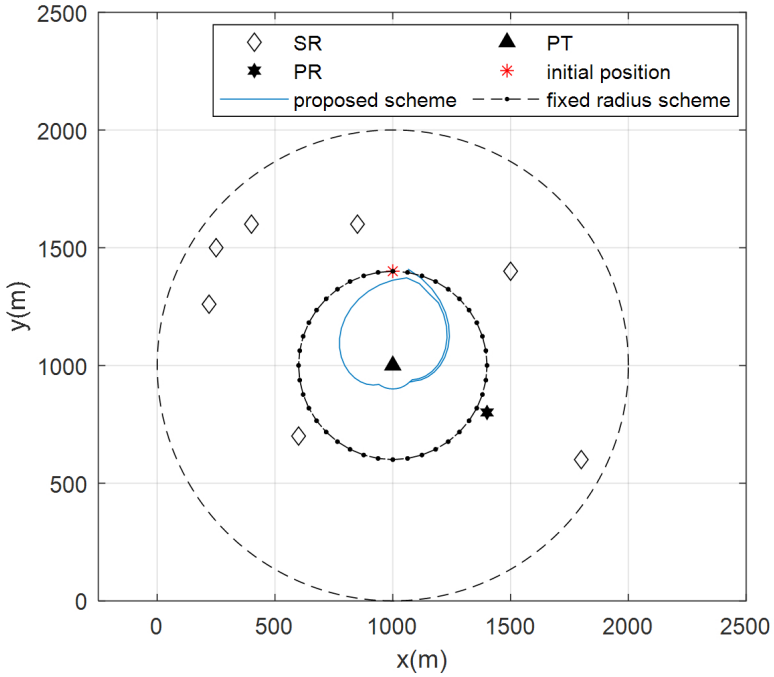


**Figure 4: The trajectory of UAV under the proposed scheme and fixed radius scheme**

reduced by the influence of $\Gamma_K$; as the UAV gradually moves away from the PR towards the SR, $R^K{}_{\max}$ gradually increases. However, influenced by the farthest distance the UAV flies within the equal flight radian and the UAV's flight towards the starting point, the UAV tends to fly relatively far away from the SR, causing $R^K{}_{\max}$ to fall again. Meanwhile, as the sensing SNR increases, it will lead to a decrease in the error probability, which enhances the sensing performance and leads to an increase in $R^K{}_{\max}$.

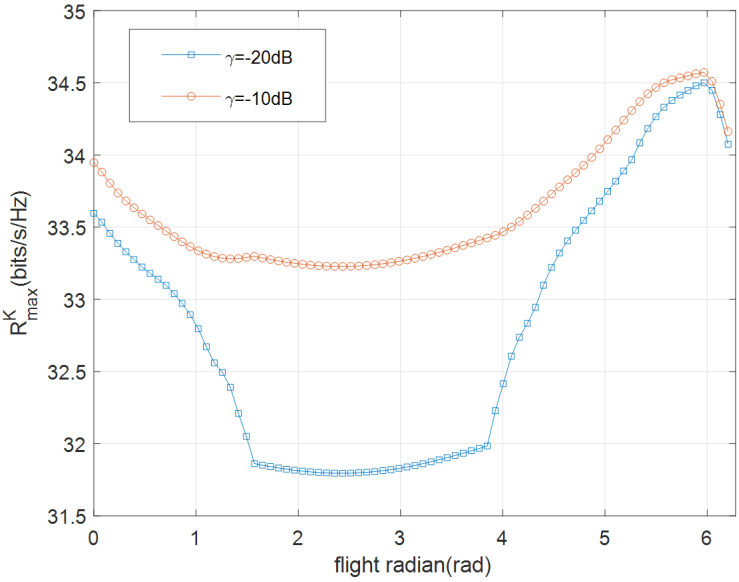


**Figure 5: The maximum throughput vs flight radian under different $\gamma$**

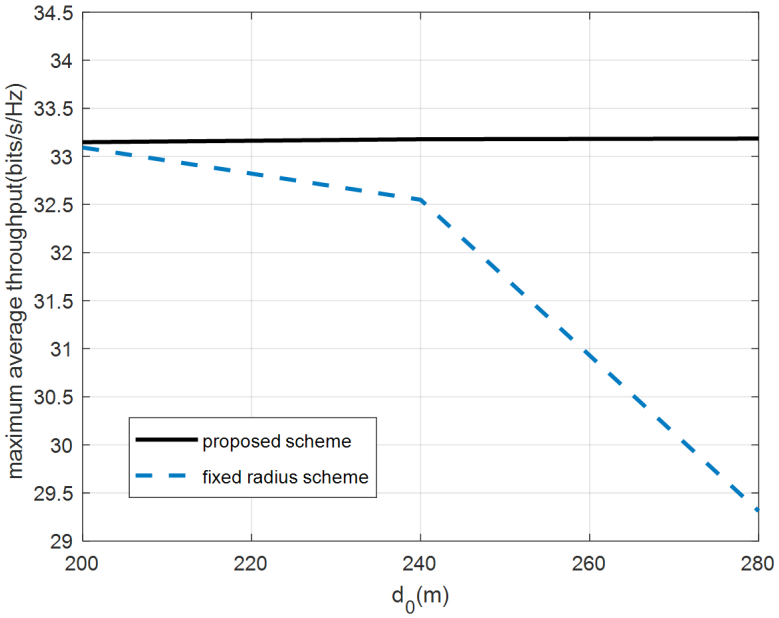


**Figure 6: Maximum average throughput vs $d_0$ under different flight schemes**

As can be seen in figure 6, the average maximum throughput under the proposed scheme is greater than that of the fixed-radius flight scheme. Combining with figure 4, it can be seen that when flying with a fixed flight radius, the UAV is close to the PR in part of the flight radian, which will result in the PR being subjected to interference from the UAV over $\Gamma_K$, thus the UAV cannot complete secondary communication during this time and then the throughput is 0. The proposed scheme in this paper, maintains the UAV secondary communication as much as possible through trajectory planning and ensures the maximum throughput for each radian $\theta$ flown by the UAV under the constraint, resulting in better performance than the fixed radius scheme.

## 5 CONCLUSION

This paper studies the SE optimization problem based on UAV trajectory planning in UAV cognitive communication network. UAV flies around PT to perform reconnaissance and detection duty, and transmits data to SR through cognitive communication. Premising the PU is not interfered by UAV, firstly, the sensing radian of UAV is optimized to maximize throughput. Secondly, on the basis of optimal sensing radian, the trajectory of UAV is planned to improve throughput. Finally, the SE optimization algorithm is proposed. Simulation results show that the proposed scheme has a better effect on protecting PU communication and improving the throughput of secondary communication than existing schemes.

## REFERENCES


[1] D. W. Matolak and R. Sun, "Unmanned Aircraft Systems: Air-Ground Channel Characterization for Future Applications," IEEE Vehicular Technology Magazine, vol. 10, no. 2, pp. 79-85, June 2015.

[2] M. J. Marcus, "Spectrum policy challenges of UAV/drones," IEEE Wireless Communications, vol. 21, no. 5, pp. 8-9, October, 2014.

[3] G. Stamatescu, D. Popescu and R. Dobrescu, "Cognitive radio as solution for ground-aerial surveillance through WSN and UAV infrastructure," 2014 6th International Conference on Electronics, Computers and Artificial Intelligence (ECAI), pp. 51-56, 2014.

[4] L. Sboui, H. Ghazzai, Z. Rezki and M. Alouini, "Achievable Rates of UAV-Relayed Cooperative Cognitive Radio MIMO Systems," IEEE Access, vol. 5, pp. 5190-5204, 2017.

[5] R. Grodi and D. B. Rawat, "UAV-assisted broadband network for emergency and public safety communications," 2015 IEEE Global Conference on Signal and Information Processing (GlobalSIP), 2015, pp. 10-14.

[6] W. Xu, S. Wang, S. Yan and J. He, "An Efficient Wideband Spectrum Sensing Algorithm for Unmanned Aerial Vehicle Communication Networks," IEEE Internet of Things Journal, vol. 6, no. 2, pp. 1768-1780, April 2019.

[7] F. Shen, G. Ding, Z. Wang and Q. Wu, "UAV-Based 3D Spectrum Sensing in Spectrum-Heterogeneous Networks," IEEE Transactions on Vehicular Technology, vol. 68, no. 6, pp. 5711-5722, June 2019.

[8] W. Xu, X. Li, C. Lee, M. Pan and Z. Feng, "Joint Sensing Duration Adaptation, User Matching, and Power Allocation for Cognitive OFDM-NOMA Systems," IEEE Transactions on Wireless Communications, vol. 17, no. 2, pp. 1269-1282, Feb. 2018.

[9] Y. Huang, J. Xu, L. Qiu and R. Zhang, "Cognitive UAV Communication via Joint Trajectory and Power Control," 2018 IEEE 19th International Workshop on Signal Processing Advances in Wireless Communications (SPAWC), 2018, pp. 1-5.

[10] Q. Wu, Y. Zeng and R. Zhang, "Joint Trajectory and Communication Design for Multi-UAV Enabled Wireless Networks," IEEE Transactions on Wireless Communications, vol. 17, no. 3, pp. 2109-2121, March 2018.

[11] H. Hu, X. Da, Y. Huang, H. Zhang, L. Ni and Y. Pan, "SE and EE Optimization for Cognitive UAV Network Based on Location Information," IEEE Access, vol. 7, pp. 162115-162126, 2019.

[12] X. Liu, M. Guan, X. Zhang and H. Ding, "Spectrum Sensing Optimization in an UAV-Based Cognitive Radio," IEEE Access, vol. 6, pp. 44002-44009, 2018.

[13] Z. Wang, F. Zhou, Y. Wang and Q. Wu, "Joint 3D trajectory and resource optimization for a UAV relay-assisted cognitive radio network," China Communications, vol. 18, no. 6, pp. 184-200, June 2021.

[14] X. Liang, Q. Deng, J. Lin and M. Huang, "Joint Trajectory Optimization and Spectrum Access for Cognitive UAV Networks," IEEE Access, vol. 8, pp. 144693-144703, 2020.

[15] Y. Liang, Y. Zeng, E. C. Y. Peh and A. T. Hoang, "Sensing-Throughput Tradeoff for Cognitive Radio Networks," IEEE Transactions on Wireless Communications, vol. 7, no. 4, pp. 1326-1337, April 2008.